LBL-12016
Preprint

Lawrence Berkeley Laboratory
UNIVERSITY OF CALIFORNIA

Materials & Molecular
Research Division

Submitted to Thin Solid Films

EROSION RESISTANCE OF CoCrAl COATINGS CONTAINING ACTIVE ELEMENT ADDITIONS

J. Maasberg, D.H. Boone, D.P. Whittle, and A. Levy

October 1981

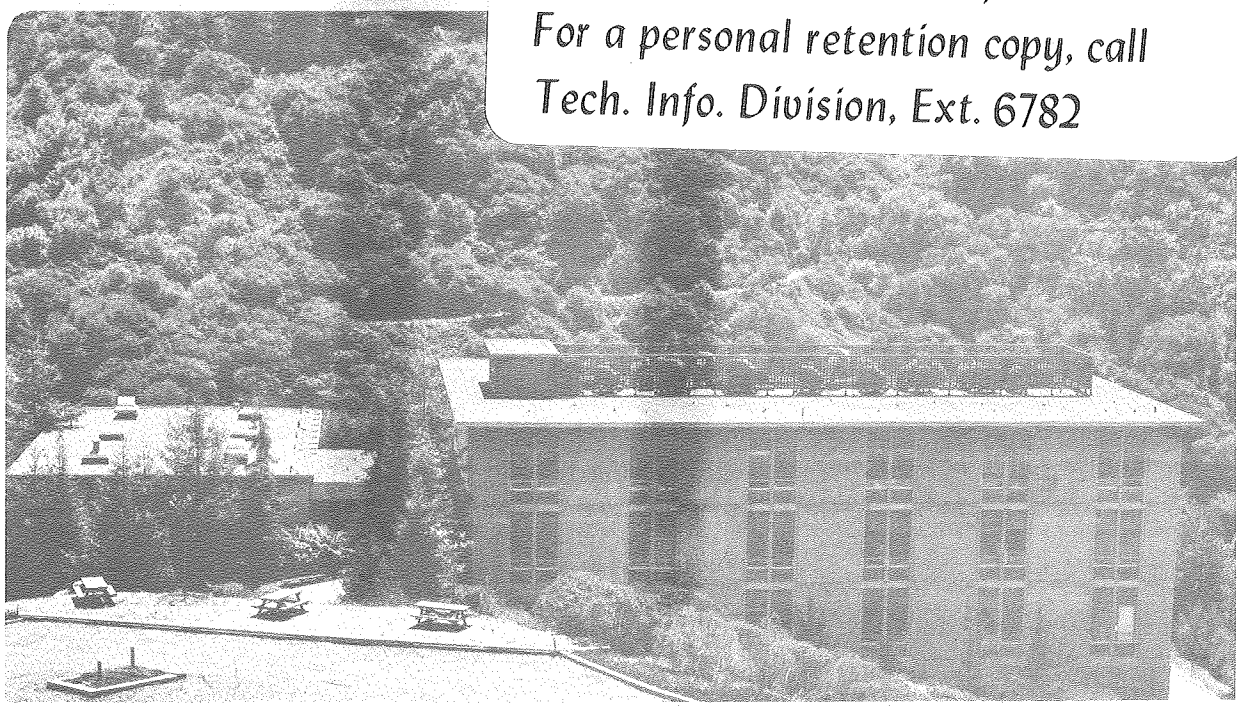

Prepared for the U.S. Department of Energy under Contract W-7405-ENG-48

DISCLAIMER

LBL-12016

EROSION RESISTANCE OF CoCrAl COATINGS CONTAINING ACTIVE ELEMENT ADDITIONS

J. Maasberg, D. H. Boone, D. P. Whittle, and A. Levy

MMRD, Lawrence Berkeley Laboratory

University of California

Berkeley, California 94720

This work was supported in part by the Director, Office of Energy Research, Office of Basic Energy Sciences, Materials Sciences Division of the U. S. Department of Energy under Contract Number W-7405-ENG-48 and by the Assistant Secretary for Fossil Energy, Office of Coal Research, Heat Engines and Heat Recovery Division of the U. S. Department of Energy under Contract Number W-7405-ENG-48 through the Battelle Memorial Institute, Pacific Northwest Laboratories, Richland, Washington.

Abstract

Materials resistant to high temperature corrosion and small particle impact erosion are necessary in the design and construction of energy conversion systems. Alumina forming MCrAl coatings with active element additions on an IN 738 substrate have demonstrated enhanced resistance to erosion damage of their oxide scales due to improved adherence of the scale. This improvement results from modifications of the scale morphology by the active element additions which encourage pegs of oxide that penetrate into the coating. Other active element additions cause a porous scale to form, increasing the erosion susceptibility. The thin alumina scales behave like a brittle material with the highest erosion rate occurring at a 90° impingement angle and scale removal occurring by a chipping action.

Introduction

Erosion of high temperature corrosion resistant materials is a significant problem encountered in energy conversion systems and, in particular, coal gasifiers. Materials and coatings designed for use in high temperature corrosive environments are dependent on the formation of continuous protective oxides. Thermal cycling induced stresses and erosion by solid particles can mechanically damage these oxides, leaving the alloy exposed to further corrosion. The addition of small amounts of reactive metals to high temperature alloys has been found to improve adhesion between the alloy and its oxide scale thereby offering resistance to thermal cycling[1]. Since these additions improve the resistance of the scale to mechanical damage, it is believed that these additions may also improve a scale's resistance to erosion.

Erosion studies on chromia forming 300 series stainless steel alloys have shown a strong correlation between the erosion rate and the scale-metal interface integrity[2]. Scales which formed pegs of oxide penetrating into the alloy had lower erosion rates than the scales on alloys which had smooth scale-metal interfaces. The highest erosion rate occurred when an internal SiO_2 formed parallel to the scale-metal interface and deteriorated scale-metal adhesion. Since the addition of active elements modifies this interface, this study was initiated to determine:

1. The feasibility of using active element additions to develop high temperature erosion resistant coatings.
2. The effect of various active elements on the coatings' susceptibility toward erosion.

3. The mechanism of scale removal for oxidized coatings with active element additions.

4. A quantization of scale adhesion in terms of erosion.

Recent erosion studies on thin oxide scales have shown that scales behave in a brittle manner, eroding at a higher rate when the particle trajectory is normal to the surface and eroding at a lower rate when the particle impacts the surface at a shallow angle. The opposite angle dependence occurs in ductile materials. Fig. 1 graphically shows the erosion behavior of ductile and brittle materials as a function of particle impingement angle[3]. The thin oxide erosion studies have shown that scale is removed by a fracturing and chipping action of the impacting particles.

Experimental

CoCrAl coatings containing single active element additions of Hf, Ti, Si, Y, Zn, or no addition were produced by electron beam physical vapor deposition EB-PVD on IN 738 substrates as detailed elesewhere[4]. Table 1 lists the coating composition and thickness for the specimens tested. The specimens were exposed to air at 1000°C for 100 h, thus forming a continuous aluminum oxide scale on the surface, and depending on the coating composition, varying amounts of internal oxidation.

The specimens were eroded at room temperature by 50 μm diameter SiC particles carried in a stream of air traveling at 200fps (60 m/s). The erosion tester used is shown in schematic form in Fig. 2. Details of the test are presented elsewhere[5]. The CoCrAl specimen was eroded at 90°, 30°, and 15° particle impingement angles in order to determine the ductile or brittle erosion behavior of the oxide. All other specimens were eroded at 30°. An

unoxidized CoCrAlY specimen was eroded in a similar manner as the oxidized specimens in order to establish the proportion of erosion due to the oxide loss as compared to coating alloy loss. The specimen weight was carefully measured after exposure to small amounts of eroding SiC particles (0.1 to 0.5g) with the resulting weight loss corresponding to the amount of erosion damage of the specimen. By dividing the erosion weight loss by the weight of SiC used to produce this loss, an erosion rate was found. Results are presented in terms of specimen weight loss per unit of erodant, i.e. erosion rate. Interrupted erosion and SEM examination was conducted to document degradation mechanism and transition from one mode to the next.

Microstructural examinations were performed on samples mounted and carefully prepared to preserve scale edges. An analytical scanning electron microscope was used to view the microstructures and identify the phases present.

Results

The weight loss vs. the amount of impacting SiC for the oxidized CoCrAl specimens is plotted in Fig. 3 and the corresponding erosion rates are tabulated in Table 2 for a 90° impingement angle. All erosion weight loss vs. weight of eroding SiC curves showed two distinct regions of erosion, the higher rate occurring initially at erodant levels below 0.3 to 0.5g SiC, and the lower erosion rate occurring between 0.5 to 3.0g SiC. During erosion testing, the oxide free metal began to appear after erosion with 0.4 to 0.6g SiC. However, significant amounts of metal did not appear until after erosion with 3.5g SiC for CoCrAlSi and CoCrAlZr, about 5.0g for CoCrAl, CoCrAlTi, and CoCrAlY, and about 11g for CoCrAlHf. The erosion of an unoxidized CoCrAlY specimen did not show any apparent weight loss until 6.0g of SiC erodant were used; thus its erosion weight loss was negligible in comparison

to the oxidized specimens. The oxidized CoCrAl specimen showed about 50% more weight loss at 30° and 15° impingement angles than at 90°.

Microstructural examinations of specimen cross-sections, Fig. 4, showed that the oxide layer varied with active element additions from continuous and non-porous to porous and non-continuous, and that the scale-metal interface varied from a smooth contact to a structure with large pegs of oxide penetration far into the metal. Generally, the CoCrAl, CoCrAlSi, and CoCrAlTi specimens had no pegs, CoCrAlY had moderate pegs, and CoCrAlHf and CoCrAlZr exhibited large well defined pegs. The CoCrAlHf oxide scale was thick and appeared dense. The CoCrAlZr oxide scale was extremely porous and easily damaged by handling. All other specimens had a continuous and apparently non-porous oxide. All specimens formed alumina, with the active elements tending to concentrate at the scale-metal interface.

Discussion

The high erosion rates observed for the oxidized CoCrAl specimen at 15° and 30° impingement angles as compared to the 90° angle indicates that the oxide scale behaves in a manner similar to a ductile material[3]. However, examination of the oxide surface during the course of erosion testing showed that the oxide was chipped and appeared to be being removed as fine chips in a brittle manner. This occurred by first removal from the higher points on the surface, then from the entire surface in the erosion zone.

As increasing amounts of metal were exposed, the erosion rate was reduced. The exposed metal appeared to be extensively deformed by the impacting particles, yet did not contribute to the erosion weight loss even after sufficient SiC to remove an oxide layer impacted the surface. This indicates that the weight losses observed for the oxidized specimens were due solely to the

loss of oxide and not metal[5]. The threshold erosion period for ductile metal substrates is significantly greater than for the brittle scales formed on them[5]. Even in this instance where the CoCrAl has a tensile ductility <0.2% at temperatures up to 600°C[6], the metal exhibited a "ductile" erosion behavior. These alumina forming specimens eroded by the same chipping mechanisms as previously studied chromia forming specimens[2], but at a much lower rate.

The susceptibility toward erosion was dependent on the type of scale-metal interface that formed and on the integrity of the oxide scale. The erosion rates are compared using the bar graphs in Fig. 4. The low erosion weight loss rates of the CoCrAlY and CoCrAlHf specimens were the result of the presence of oxide pegs which penetrated deeply into the alloy and apparently helped to strengthen the scale-metal interface. The discontinuities in weight loss for the Hf addition to CoCrAl were due to larger chunks of oxide being broken off periodically. Pegs were absent on the CoCrAlTi and CoCrAlSi specimens and the corresponding erosion weight loss of these coating scales was higher. The CoCrAlZr specimen formed pegs, yet exhibited the highest erosion rate among the specimens studied. Zr affected the scale growth in such a manner as to form a high degree of porosity in both the pegs and the scale. This porous, friable scale had little resistance to any form of mechanical damage and required extremely careful handling to avoid damaging the scale. The very high initial weight loss rate of the CoCrAlZr specimen was attributed to oxide particles, possibly cobalt oxide, present on the surface which were easily knocked off by the first few impacting SiC particles. Fig. 5 shows schematically the ease of erosion as a function of the morphology of the scale-metal interface[2]. The reason for this behavior is speculative

as the scale did not separate at the scale-metal interface upon impact by the eroding particles. Rather it was removed in layers by a cracking and chipping mechanism. It is reasoned that the increased ability of the pegged scales to transmit a portion of the force of the impacting particles into the more ductile substrate reduces the erosivity of the particles and, therefore, decreases the amount of erosion in the pegged scales.

An attempt was made to use this test and the results as a more quantitative measure of scale adherence. The results are presented in Table 2 with time to first observation of oxide free metal reported. For a dense scale, adherence as measured by time to first removal by eroding particle was found to be in agreement with visual and metallographical results and could possibly be used to identify differences in, for example, active element level within a series of tests.

The CoCrAl specimen which did not form pegs had an unexpectedly low initial erosion rate. The continuous, dense, and thick nature of this scale compared to the scales formed on the active element addition CoCrAl's may have contributed to its erosion resistance. Deep etching examination of the CoCrAl oxide by Whittle, et al.[7] has shown that there was a slight pegging effect for this specimen due to diffusion of Ti from the substrate through the coating to the scale-metal interface. It is also possible that the active element levels investigated in this study are above the optimum level for maximum adherence and lower levels would show further improvements over the CoCrAl specimen. This behavior is being further investigated as it has a significant impact on the need for active element additions to CoCrAl protective coatings where erosion rather than thermal cycling is involved.

Conclusions

From this experiment, it can be concluded that:

1. Small amounts of active element additions have a substantial effect on the microstructure of the scale and its erosion rate.
2. The occurrence of pegging of the scale at the scale-metal interface increases the erosion resistance of the scale, particularly the Hf and Y active element additions.
3. Ti and Si additions formed a smooth contact between the scale and the metal and were associated with a higher erosion rate.
4. Zr encouraged pegging but caused the scale to become porous and lose its integrity, thereby forming a non-protective, easily eroded scale.
5. The coating without additions had a smooth interface, yet it exhibited a low erosion rate. This could be due to the greater integrity of the scale morphology and/or to small amounts of titanium oxide at the interface which diffused from the substrate material.
6. The oxide scales eroded in a brittle manner by a cracking and chipping mechanism.

Acknowledgements

This work was supported in part by the Director, Office of Energy Research, Office of Basic Energy Sciences, Materials Sciences Division of the U. S. Department of Energy under Contract Number W-7405-ENG-48 and by the Assistant Secretary for Fossil Energy, Office of Coal Research, Heat Engines and Heat Recovery Division of the U. S. Department of Energy under Contract Number W-7405-ENG-48 through the Battelle Memorial Institute, Pacific Northwest Laboratories, Richland, Washington.

References

1. D. P. Whittle, J. Stringer, "Improvements in High Temperature Oxidation Resistance by Additions of Reactive Elements or Oxide Dispersions", Proceedings from International Conference on "Residuals, Additives and Materials Properties", The Royal Society, London (1978).

2. J. A. Maasberg, A. V. Levy, "Erosion of Elevated Temperature Corrosion Scales on Metals", to be published in Wear.

3. I. Finnie, "Erosion of Surfaces by Solid Particles", Wear 3 (1960).

4. D. H. Boone, S. Shen and R. McKoon, "Electron Beam Evaporation of Low Vapor Pressure Element in MCrAl Coating Compositions", Thin Solid Films, 63 (1979) 299-304.

5. G. Zambelli and A. V. Levy, "Particulate Erosion of NiO Scales, Wear, 68 (1981) 305-331.

6. D. H. Boone and G. W. Goward, "The Use of Nickel-Aluminum Intermetallic Systems as Coatings for High Temperature Nickel Base Alloys", Proceedings of 3rd Bolton Landing Conference on Ordered Alloys, Baton Rouge, Claitor's (1970) 545-564.

7. D. P. Whittle, D. H. Boone, I. M. Allam, "Morphology of Al_2O_3 Scales on Doped Co-Cr-Al Coatings", Thin Solid Films, 73, 359-364 (1980).

Table 1
Composition of Coatings

Thickness (um)	Cobalt	Chromium (wt.%)	Aluminum (wt.%)	Active element (wt.%)
120	Balance	28.3	10.7	0
125	Balance	20.1	10.1	4.9 Y
100	Balance	24.0	9.0	1.6 Si
135	Balance	20.8	9.6	3.6 Ti
100	Balance	19.6	8.8	6.6 Zr
120	Balance	23.0	9.0	1.4 Hf

Table 2
Erosion Data

Coating	Weight loss after 0.3g SiC (mg)	Initial erosion rate (mg/g-SiC)	Oxide thickness (m)	g of SiC to reach metal (g)	Interface
CoCrAl	0.7	1.3	8	4.5	smooth
CoCrAlHf	0.8	1.3	2	11.0	pegged
CoCrAlY	0.5	1.3	3	5.5	pegged
CoCrAlSi	1.6	4.2	10	3.5	smooth
CoCrAlTi	1.9	6.3	4	6.0	smooth
CoCrAlZr	3.2	14.0	14	3.5	pegged

Figure Captions

Figure 1. Erosion vs. impingement angle for ductile and brittle materials[3]

Figure 2. Schematic drawing of gas-particle erosion apparatus

Figure 3. Erosion weight loss as a function of increasing weight of eroding particles

Figure 4. Metallographic cross sections of oxidized CoCrAl (active element addition) specimens shown with weight loss after erosion with 3.0g SiC

Figure 5. Schematic drawings of scale-metal interfaces

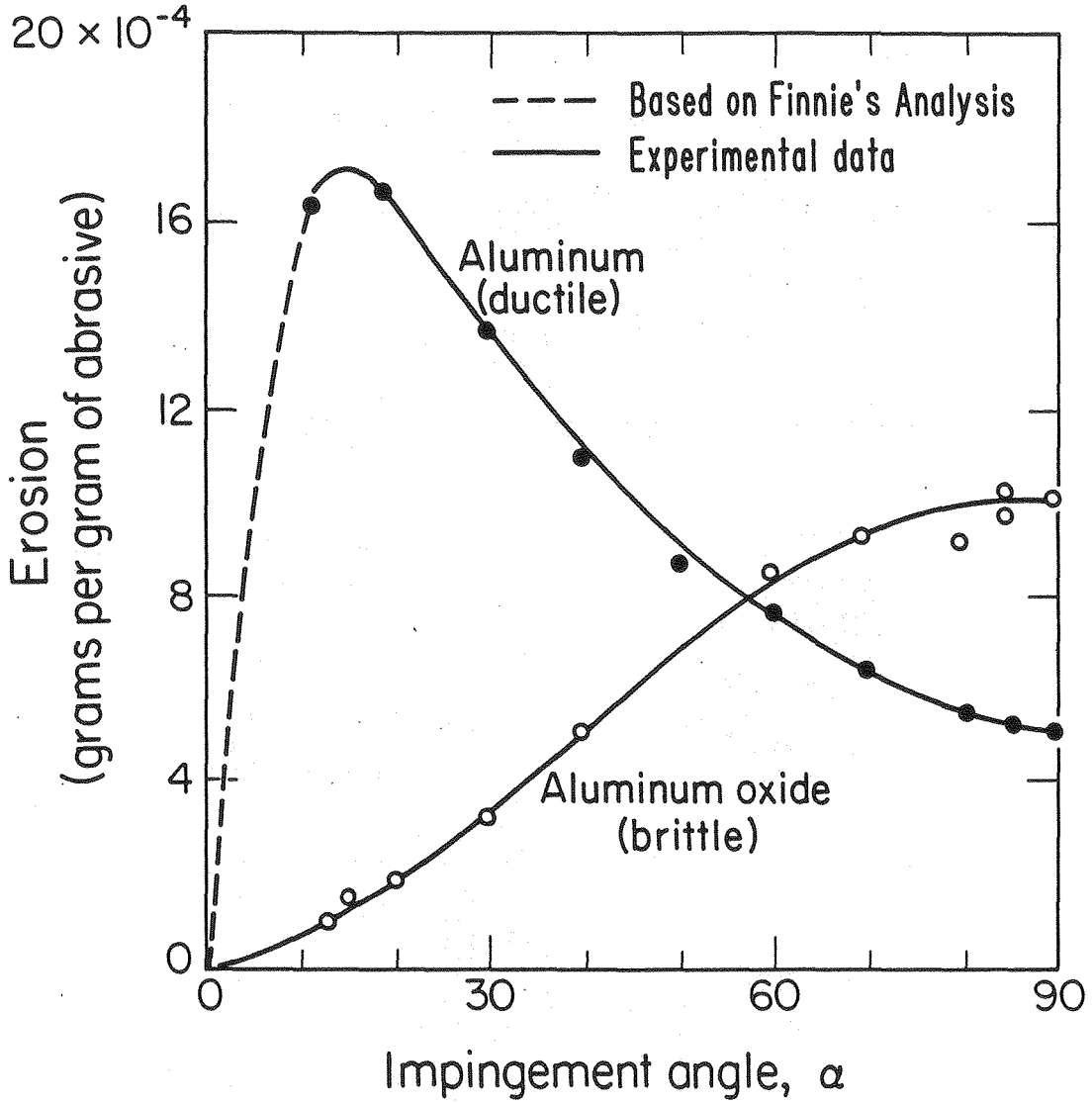

Figure 1

XBL 793-974

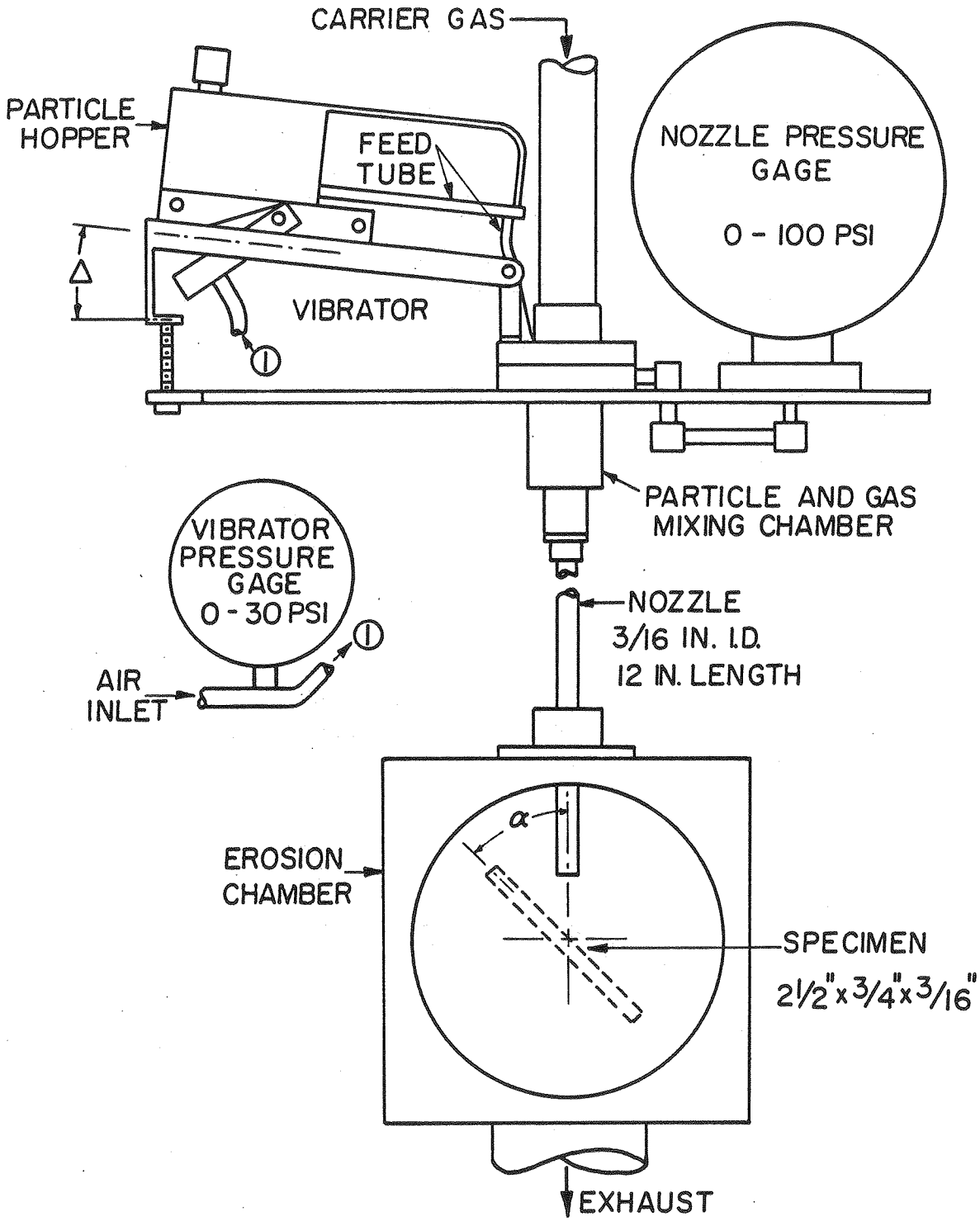

Figure 2

XBL775-5525

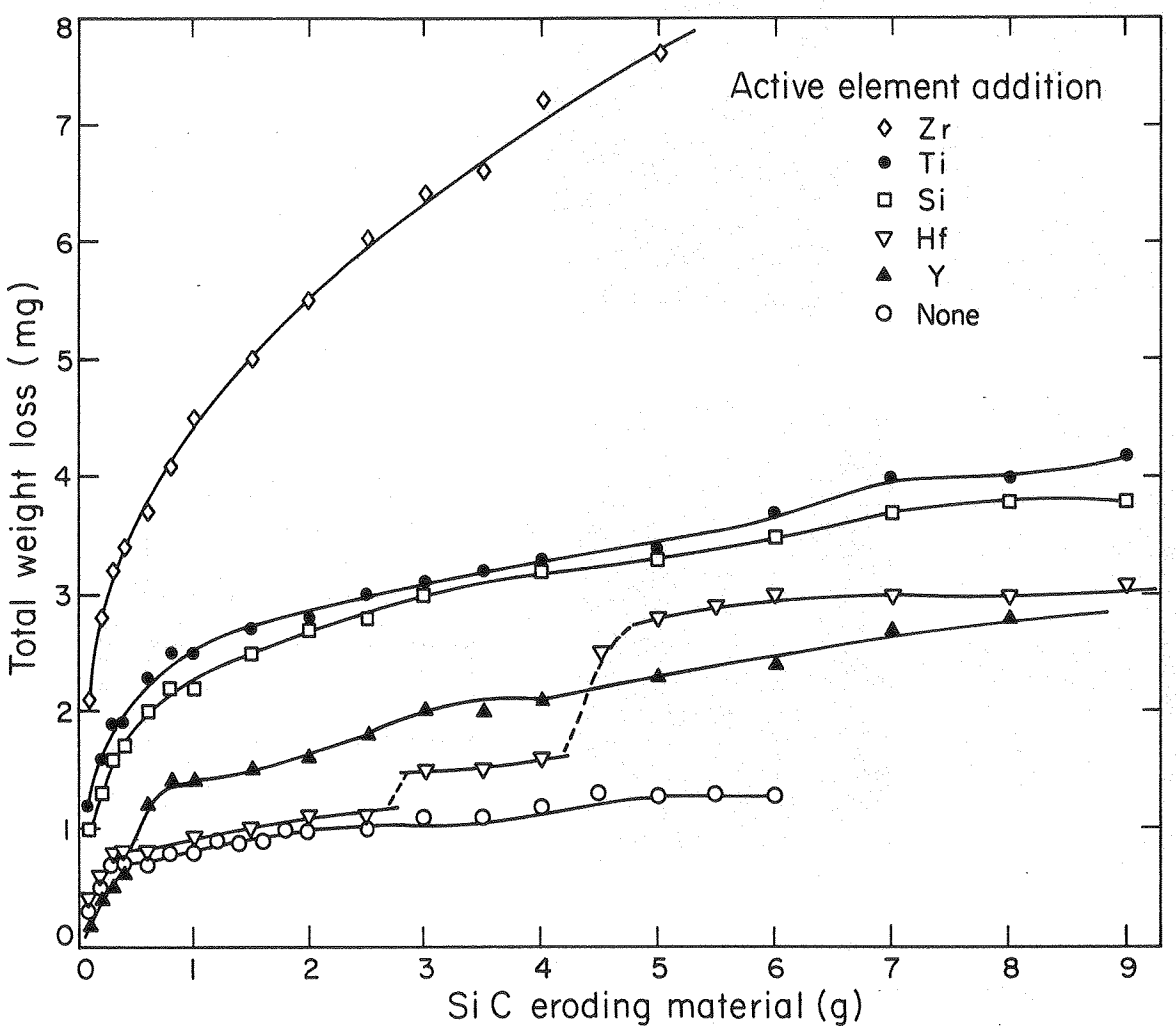

Figure 3

XBL 814-709

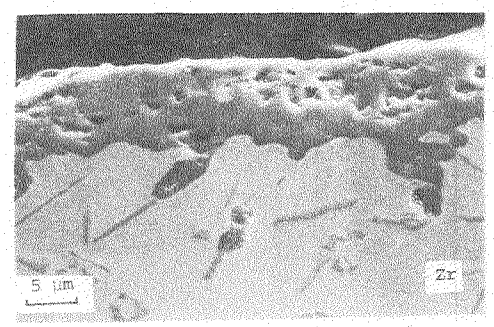

scale lacks integrity

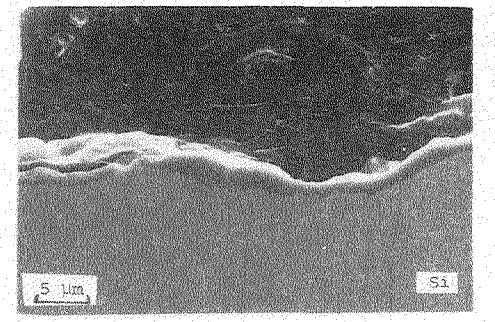

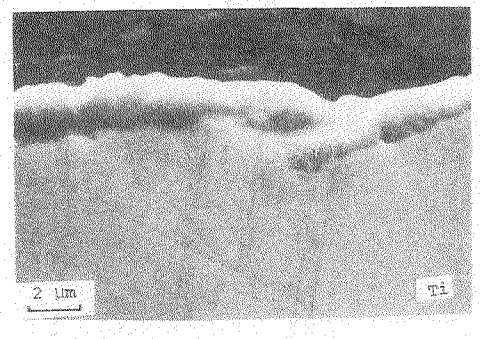

lack of oxide pinning

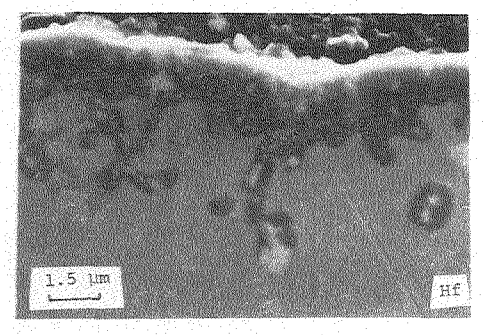

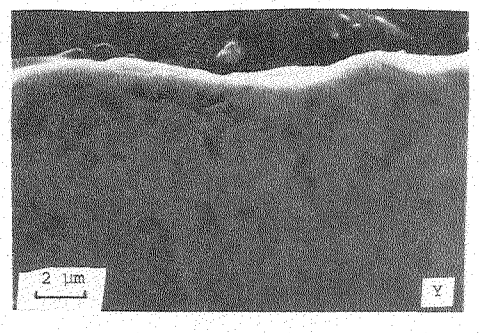

oxide pinning

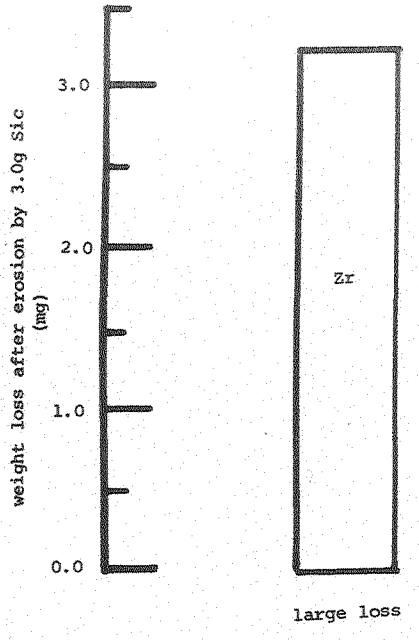

large loss

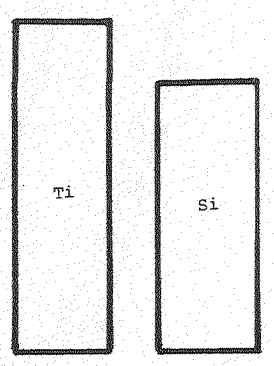

moderate loss

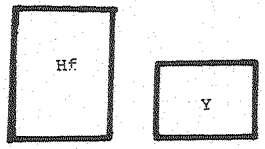

small loss

Figure 4

XBB 809-10348

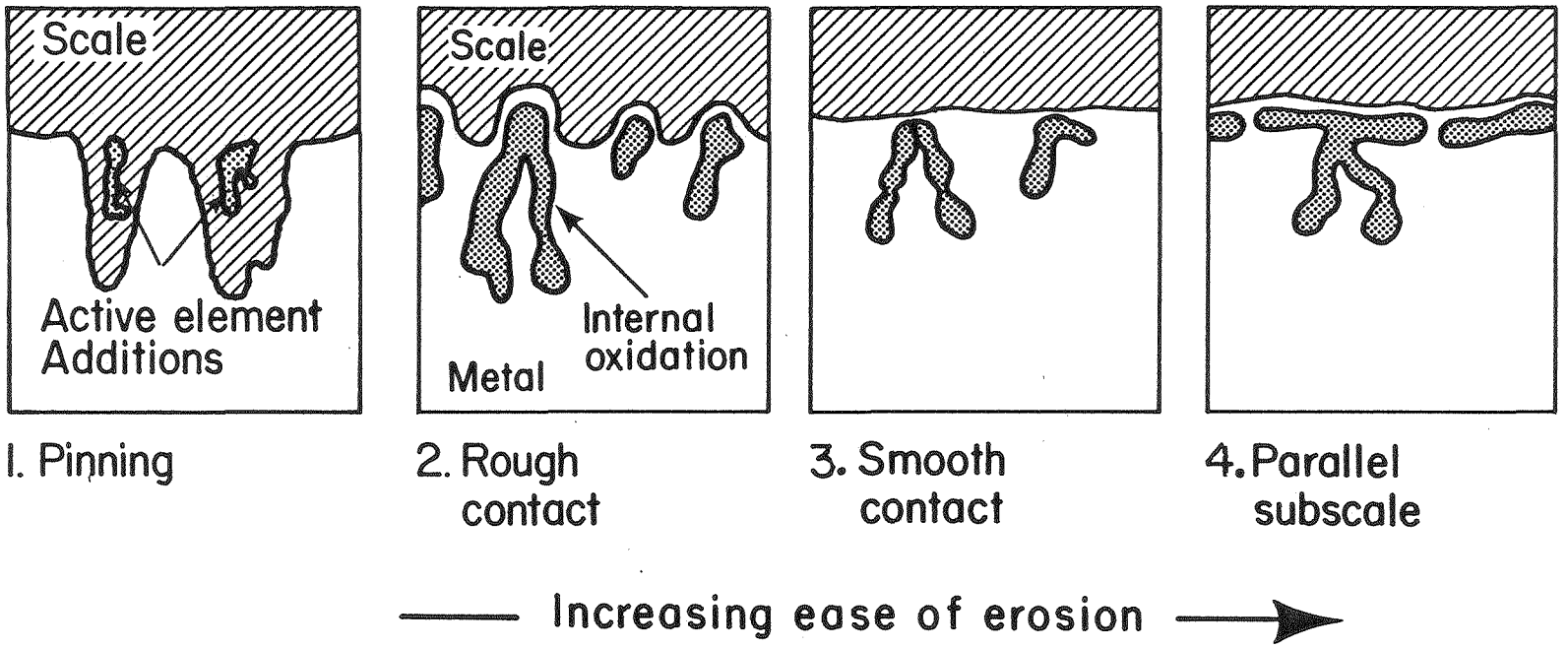

Figure 5

XBL 7912-13356A